Original Paper

Experiment and Analysis of Spinning Membrane Deployment Focusing on Shape Imbalance for Solar Sail

By Kengo Shintaku[1], Saburo Matunaga[1,2], Go Ono[3], Hiraku Sakamoto[1],
Takeshi Satoh[1], Osamu Mori[2], Yoji Shirasawa[2] and Nobukatsu Okuizumi[2]

[1]*Tokyo Institute of Technology, Tokyo, Japan*
[2]*JAXA, Sagamihara Japan*
[3]*The University of Tokyo, Tokyo, Japan*

The small solar power sail demonstrator IKAROS was developed and launched in 2010 by JAXA and deployed its large membrane successfully. Through IKAROS's on-orbit operation, one of the most critical problems was a sail's shape imbalance during the sail deployment sequence. This paper focuses on the evaluation and consideration of the sail's imbalance through high vacuum experiments using a scale-down sail model. The experimental results obtained using the specially designed rotating mechanism and a small scale model lead to a hypothesis of the reason for the IKAROS's imbalanced deployment. The experimental results are extrapolated up to IKAROS's scale, using dimensionless analyses.

Key Words: Solar Sail, High Vacuum Experiment, Membrane Deployment

Nomenclature

L : tip mass rotating radius
θ : tip mass angle
l : length of sail
F : centrifugal force
D : bending stiffness of membrane
dl : folding width
n : number of folding
E : Yong's modulus
t : thickness of membrane

1. Introduction

Japan Aerospace Exploration Agency (JAXA) launched a solar power sail demonstrator "Interplanetary Kite-craft Accelerated by Radiation Of the Sun (IKAROS)" on May 21, 2010. This spacecraft demonstrated several essential technologies required for the future solar power sail exploration mission toward Jupiter and Trojan asteroids[1,2]. One of the essential technologies demonstrated by IKAROS is the deployment of a large membrane (thickness: 7.5µm, radius: 20m) in space. After the deployment operation was performed, successful full- deployment of the sail membrane was confirmed by a picture taken by a small deployable camera, as shown in Fig. 1.

The sail is square in shape, which consists of four trapezoidal petals. The folding line of each petal is normal to the direction of centrifugal force. One mass is attached at the corner of the square (total four masses) by tethers to increase the centrifugal forces acting on the membrane, and the inertial momentum of the sail. The sail is connected to the main body by tethers so as not to collide with the main body during the sail deployment sequence.

IKAROS is a spinning type solar sail, in which the membrane is deployed and maintained flat by centrifugal force. Fig. 2 shows the deployment method of the membrane of IKAROS. The deployment sequence is divided into two major stages. In the first stage, four rolled-up petals are extracted like a Yo-Yo despinner, to form a cross shape held by rotating stopper guides. In the second stage, these guides are released, and the four petals are extended to form a square shape. At the first stage, the deployment is performed quasi-statically. On the other hand, the second stage deployment is performed dynamically.

This deployment method is expected to be realized with simpler and more lighter-weight mechanism than other deployment methods, because it does not require compressive structural members. This method, however, has a risk of instability of the main body's attitude and/or the membrane's behavior. But it is very difficult to investigate the dynamics of membrane on ground because of air drag and gravity force.

Through IKAROS's on-orbit operation, it was found that one of the most critical problems was a shape imbalance after the first stage deployment. The shape imbalance means deflection with regard to the symmetric reference shape. Fig. 3 shows images taken by four monitor cameras mounted on the main body of IKAROS, after the first stage deployment. From an image analysis, the deflection of each sail against the ideal cross shape is shown in Table 1.

In the second stage deployment, the monitor camera images and the gyroscope data show that one of the petals of sail is got delayed to deploy about 27 seconds. The gyroscope data (Fig. 4) shows that the center of oscillation is changed around 27 second. And at this time, it is found that one of the sail between CAMERA1 and CAMERA2 has not been deployed

yet (Fig. 5).

This paper focuses on the consideration and evaluation of shape imbalance of an IKAROS-type solar sail. It aims at clarifying the cause and effect of shape imbalance. To achieve this purpose, the high vacuum experiments using scale-down sail model are conducted, and the results are extrapolated up to the IKAROS size using dimensionless analyses. From the dimensionless analyses, the differences between experiment on the ground and IKAROS are discussed. These approaches identify the possible reasons of shape and deployment imbalances observed in IKAROS, and pave the way for further detailed analysis.

Fig. 1.   The solar sail demonstrator, IKAROS.

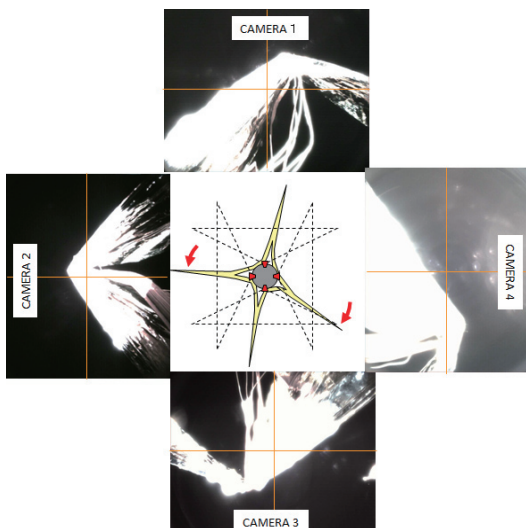Fig. 2.   IKAROS's membrane deployment sequence.

Fig. 3.   Monitor camera images after the first stage deployment.

Table 1.   Sail deflection against the ideal cross shape.

CAMERA	1	2	3	4
Deflection	5.1deg	0.6deg	2.7deg	-26.7deg

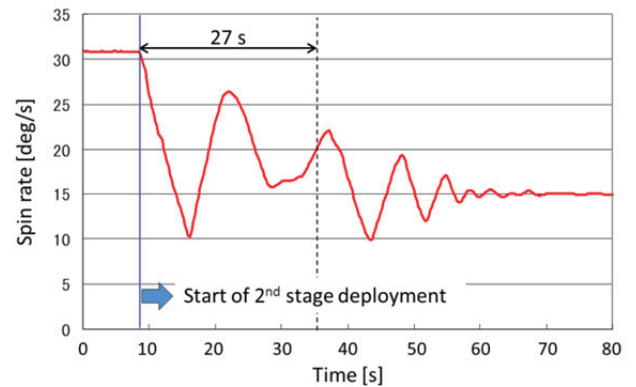(Positive direction is the same as rotational direction of IKAROS)

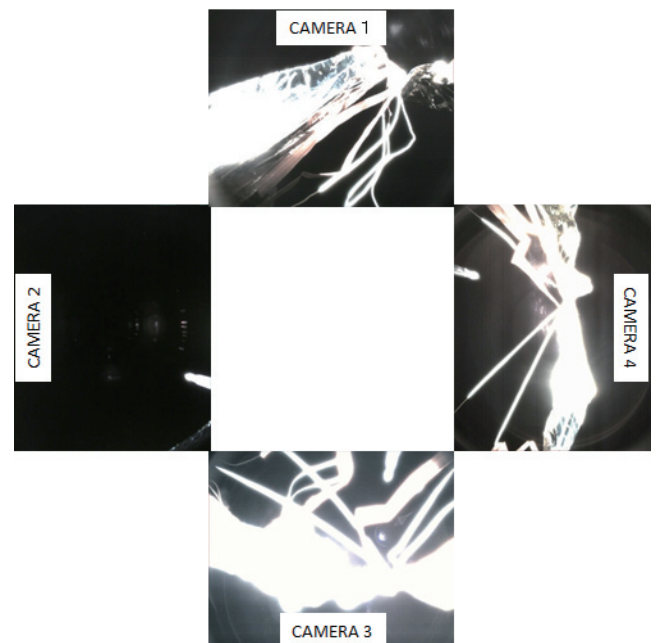Fig. 4.   Gyro scope data at second stage deployment.

Fig. 5.   Monitor camera images taken at 27 seconds after the start of the second stage deployment.

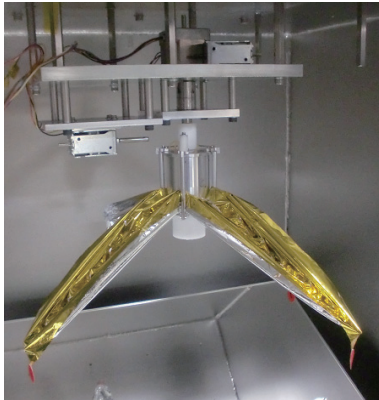## 2.   Experimental Equipment and Evaluation Parameters

A vacuum chamber and a deployment system used in the membrane deployment experiment are shown in Fig. 6. A motor is connected to a cylinder to spin the sail model. A small-scaled model is set to this cylinder. The cylinder has four stopper guides and link joints to hold the sail model. When the cylinder is rotating, a solenoid is turned on and solenoid's bar pushes the link joints, then the four stopper guides are released. Finally, the sail is deployed.

The deployment system is placed in the vacuum chamber. A large mirror is placed under the deployment system on the bottom of the vacuum chamber. It reflects the model's dynamic motion, and a high-speed camera outside the vacuum chamber records a movie of the model behavior. From the movie, 3D position of the tip masses are measured by a

homography transform and parameters for evaluation are obtained. All the tip masses are numbered as ID 1~4. Then two parameters for evaluation are set as tip mass rotating radius, L, and tip mass angle, θ, as shown in Fig. 7. The tip mass rotating radius, L, is the distance from the center of rotation to the each tip mass. And the tip mass angle, θ, is defined as the angle between the each tip mass. If the all tip mass angles are 90 degree, the sail shape is an ideal balanced shape.

(a)   Vacuum chamber

(b)   Deployment system

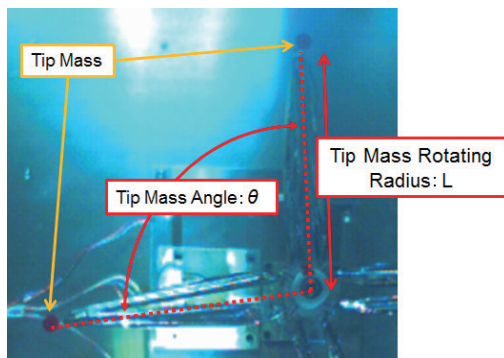Fig. 6.   Experimental equipment.

Fig. 7.   Evaluation parameters.

3.   First Stage Deployment Experiment

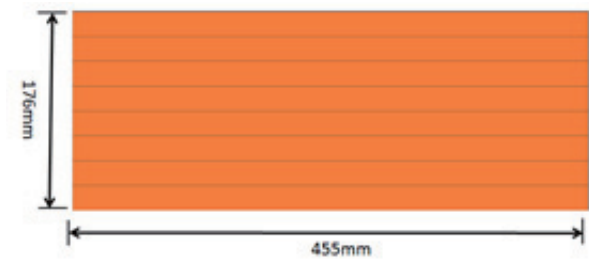### 3.1.   Experimental Methods

In this experiment, scale-down sail models are attached to the deployment system and are spun around the hub. The cross shape after the first stage deployment are evaluated using the tip mass's position.

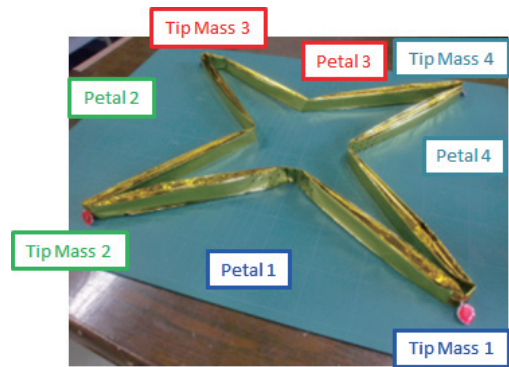A scale-down sail model adopted in the experiment is

shown in Fig. 8. Although IKAROS's membrane consists of four trapezoidal petals, this model consists of four rectangle petals, shown in Fig. 8(a), to simplify the motion phenomena. The membrane is made of polyimide film of 7.5μm in thickness, which is the same with IKAROS. The four rectangle petals are Z-folded respectively, and the edges of the Z-folded bundles are connected to form the configuration shown in Fig. 8(b). Please note that this simplified rectangular model cannot deploy the folded membranes.

Two boundary conditions between the sail and the stopper guide are considered in the experiments. Fig. 9(a) shows a constraint free condition that the sail can slide over the stopper guide. On the other hand, in a constraint condition (Fig. 9 (b)), the sail cannot slide at all by a fixture.

Spinning rate of the model ranges from 3Hz at the start of the experiment and up to 6 Hz continuously. After that the spinning rate is slowed down to 3Hz again as shown in Fig. 10. The measurement by the high speed camera is started more than 20 seconds after the motor begins to rotate in a constant speed. The experiments with each condition were repeated three times to confirm the reproducibility of the motions.
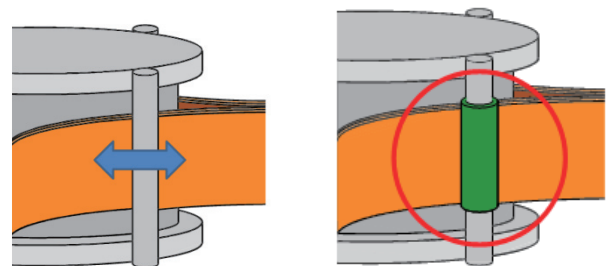

(a)   Size of rectangle petal

(b)   Scale-down model with four rectangle petals

Fig. 8.   Scale-down sail model for the first stage deployment experiment.

(a)   Constraint free condition   (b) Constraint condition

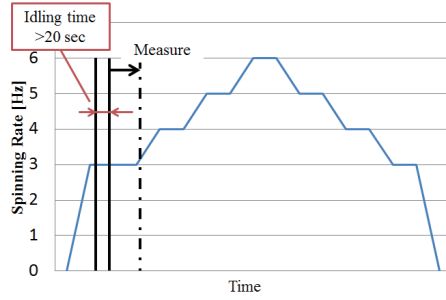Fig. 9.   Boundary conditions between sail and stopper guide.

Fig. 10.   Spinning rate operation.

3.2.   Experimental results

One of the results of the three-time repeated experiments for each condition is shown in Fig. 11 and Fig. 12. Only one typical result is shown for each condition respectively because qualitatively similar results were obtained in the three times.

The tip mass rotating radius is almost constant in both the constraint and constraint-free condition. Each tip mass angle value approaches to ideal 90 degree when spinning rate became faster in both experimental conditions. As shown in the red colored line in Fig. 11, and the blue colored line in Fig. 12, the tip mass angle does not approach to 90 degree perfectly and left about 10 degree deflection with respect to the ideal position. In case of the constraint condition, the tip mass angle is decreased gradually when spinning rate became slower. On the other hand, in case of constraint free condition, it keeps almost constant value.
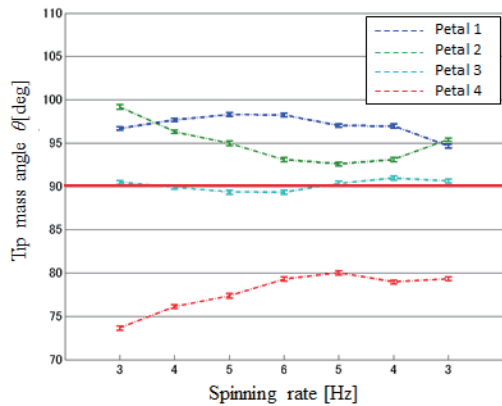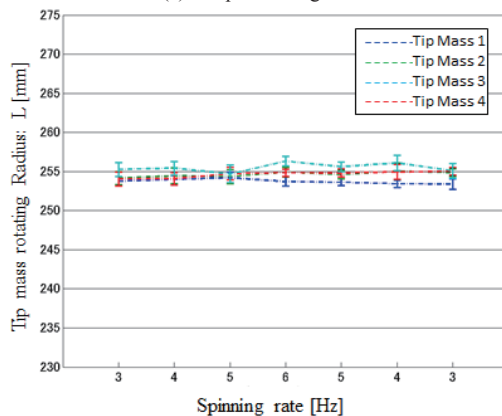

(a)   Tip mass angle θ

(b)   Tip mass rotating radius L

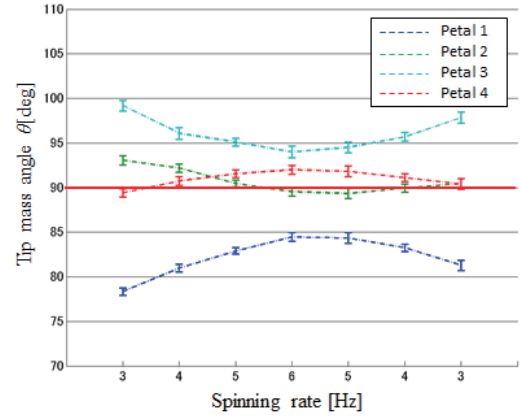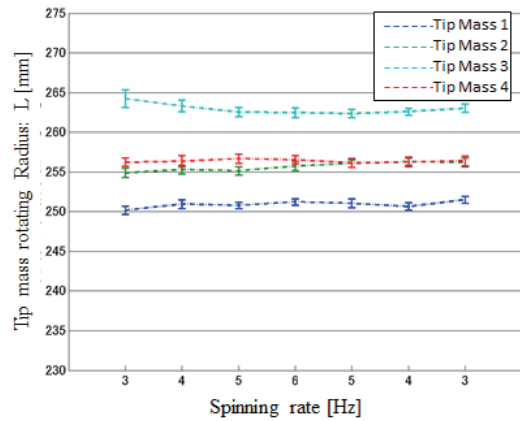Fig. 11.   Experimental results under the constraint free condition for variable spinning rate.

(a)   Tip mass angle θ

(b)   Tip mass rotating radius L

Fig. 12.   Experimental results of constraint condition for variable spinning rate.

3.3.   Discussion and dimensionless analysis

In the ideal condition, the all tip mass rotating radiuses should be the same length. But actually it is difficult to keep all the sail length strictly same in the experiment. So the each sail has a different length from the ideally designed one at the initial condition.

Let consider the sail be modeled as two simple tethers in Fig. 13, the cross shape after the first stage deployment is determined by the tether's length $L1$ and $L2$ geometrically. When $L1$ is shorter than $L2$ by 3 mm, the tip mass is deflected from the nominal position by 10 degrees. In case of the fastest spinning rate in the experiment, the tip mass angle does not approach perfectly to the ideal position. By considering accuracy of the experimental equipment, this deflection is considered as reasonable and proper due to the sail length non-uniformity between $L1$ and $L2$. In addition, when the spinning rate is fast enough, the shape imbalance after the first stage deployment is due to the sail length non-uniformity.

Next, in order to consider the similarity rule between IKAROS and the experimental model, a dimensionless number π_1 is defined as a ratio of the bending stiffness effect that constricts the deployment, to the centrifugal force that helps the deployment as shown in Eq. (1).

$$\pi_1 = \frac{\left(\dfrac{D \times l}{dl}\right)}{\left(F \times dl\right)} \tag{1}$$

The numerator represents the effect of bending stiffness of the membrane. D is the bending stiffness of the membrane as a thin-plate, and l is the membrane length and dl is the folding width. The denominator represents the moment due to the centrifugal force that acts to open the folding lines. Here the centrifugal force F is assumed to be provided only by tip masses, since the mass of the membrane is significantly smaller than the tip masses, and dl is selected as the characteristic length to consider the scale factor between experimental models and IKAROS. Detailed expressions of D and F used in the following analysis are shown in Appendix A.

The dimensionless number π_1 in the experimental condition and IKAROS's case are plotted in Fig. 14, and it is found that the effect of centrifugal force in the on-orbit IKAROS may be very larger than that under the experimental condition. Thus, in case of IKAROS, the centrifugal force may affect to the cross shape after the first stage deployment. And it is concluded that the main cause of the shape imbalance in IKAROS was possibly the sail length non-uniformity.
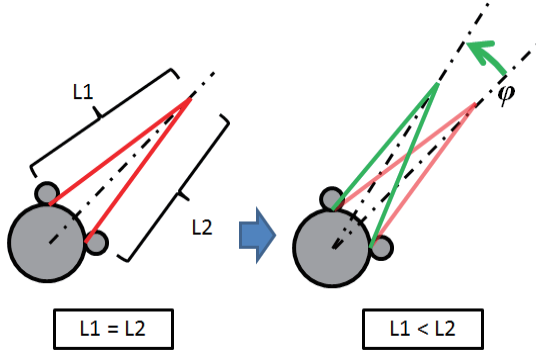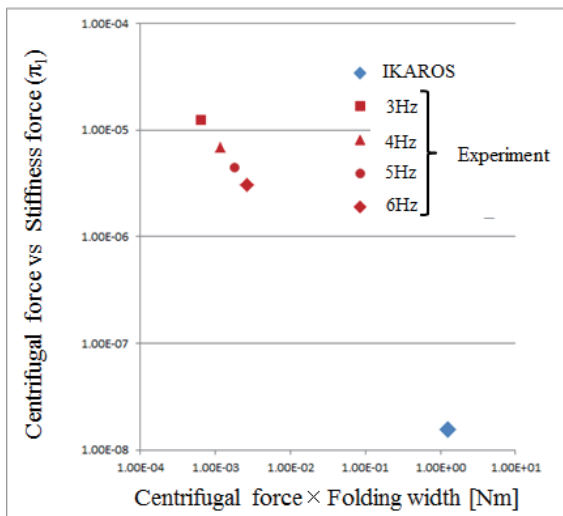

Fig. 13.   Tether model.

Fig. 14.   Dimensionless number π_1 for the first stage deployment experiment.

4.   Second Stage Deployment Experiment

4.1.   Experimental methods

Three scale-down sail models are prepared for the second stage deployment as shown in Table 2, and Model 1 is shown in Fig. 15. The second stage experiments were conducted form relatively balanced cross shape initial condition. In addition to it, Model 1 is deployed from imbalanced cross shape as shown in Fig. 16. The initial tip mass angles for petals 2 and 3 were set as approximately 70 degrees. The spinning rate was set at 3, 4, 5, and 6 Hz. Experiments were repeated three times for each conditions to confirm the reproducibility of the results.

Table 2.   Feature of scale-down model.

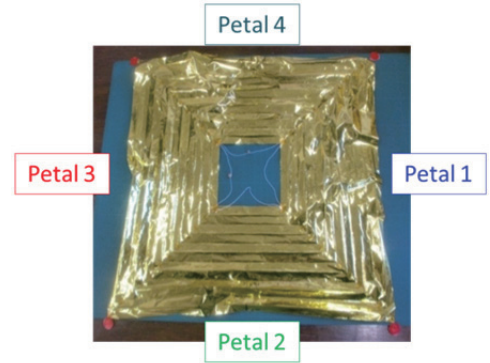|	Model 1	Model 2	Model 3
Size	455mm×455mm		
Tip mass weight	0.3 g		
Membrane thickness	7.5μm	7.5μm	25μm
Folding width	22mm	14mm	22mm

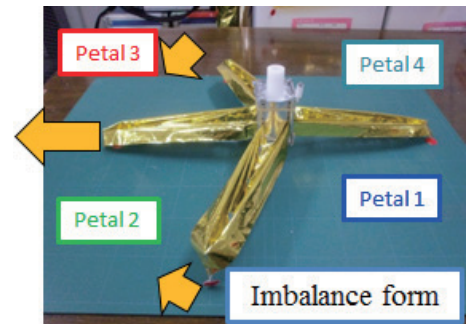Fig. 15.   View of the small model (Model 1).
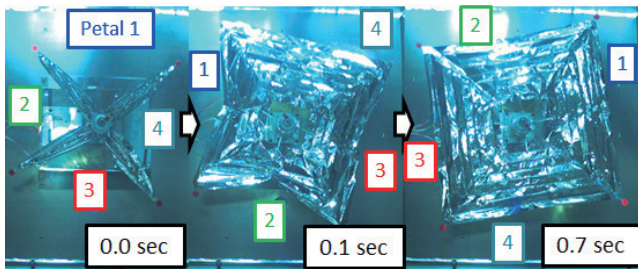

Fig. 16.   Imbalance cross shape.

4.2.   Experimental results

Some examples of the experimental results are shown herein. Fig. 17 shows the images of deployment experiment and Fig. 18 shows the results about the tip mass angle. From Fig. 17 (c), the petal 1 and the petal 4 are already deployed completely at 0.1 second. On the other hand, the petal 2 and the petal 3 are on the middle of deployment process at that time. The petal 2 and the petal 3, which are got delayed to deploy, have significantly small tip mass angle values before the second stage deployment. This tendency was true in other two repeated experiments. This is possibly because of "the double folding" as shown in Fig. 19 that exists around the
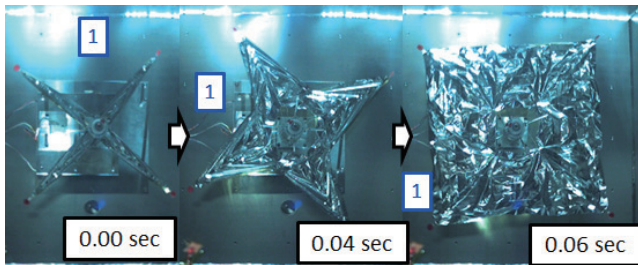
stopper guide before the second stage deployment. Due to the double folding effect of the sail, the sail's deployment may have been interfered. The less the tip mass angle at the initial condition is, the more the sail's deployment is interfered as shown in Fig. 20.

On the other hand, from Fig. 17 (a) and Fig. 18 (a), the petals where the tip mass angles are relatively large value before the second stage deployment are delayed to deploy. In the same experimental condition, the same petal 1 is delayed to deploy. It is concluded that this is because of plastic creases along the fold lines on the membrane.
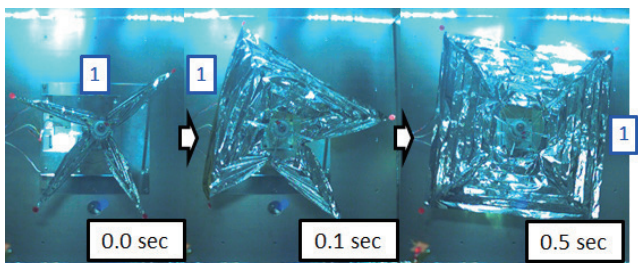
From Fig. 17 (b) and Fig. 18 (b), when the sail is rotated fast, the all petals are deployed at the approximately same time. In the experiments with Model 1, when the spinning rate was set at faster than 4 Hz, the all petals are also deployed at the approximately same time for all three repeated experiments. When the sail is rotated fast enough, the second stage deployment is not affected by stiffness of the double folding or fold crease.

(a)   3Hz, spinning deployment from a balanced shape

(b)   6Hz, spinning deployment from a balanced shape

(c)   3Hz, spinning deployment from an imbalanced shape
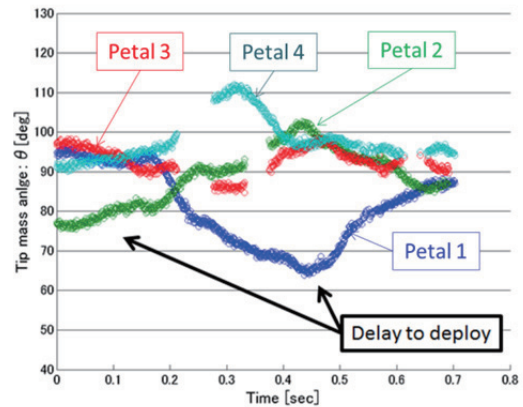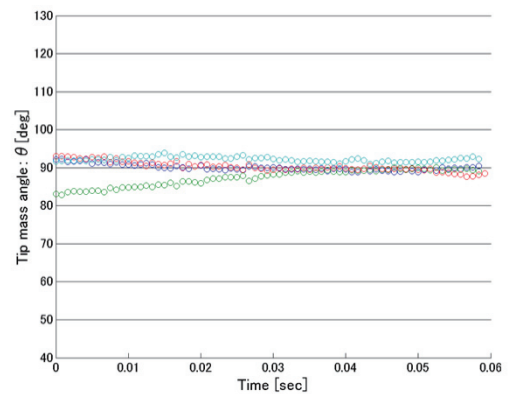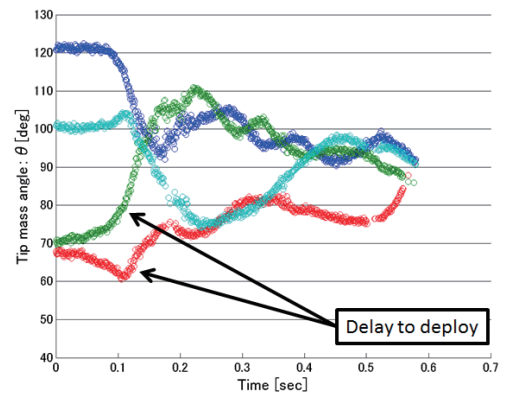Fig. 17.   Images of the second stage deployment experiment.

(a)   3Hz, spinning deployment from a balanced shape
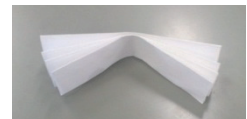

(b)   6Hz, spinning deployment from a balanced shape

(c)   3Hz, spinning deployment from an imbalanced shape
Fig. 18.   Tip mass angle results of Model 1.

(a)   Z folding   (b) Double folding
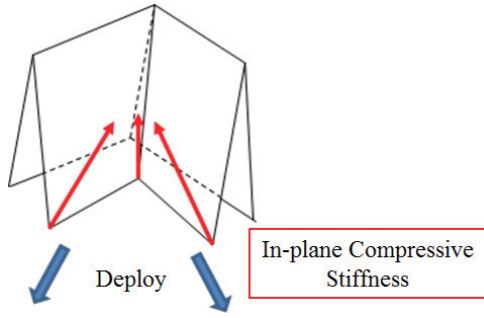Fig. 19.   IKAROS's membrane folding methods.

Fig. 20.   Effect of double folding.

4.3.   Dimensionless analysis

In order to consider the similarity rule, a dimensionless number π_2 is defined as ratio of the force due to the crease's stiffness that constricts the deployment to the centrifugal force that helps deployment, as shown in Eq. (2).

$$\pi_2 = \frac{F}{n \times \alpha E \times t \times dl} \tag{2}$$

In the numerator, F, is the centrifugal force. In the denominator, n is the number of the folds, and the rest of the term represents the compressive stiffness of the post-buckled membrane, where t is the thickness of the membrane. αE is the equivalent compressive stiffness of the membrane calculated by solving a membrane's post-buckled problem approximated to Elastica problem, as shown in Fig. 21.[4] Please note that the term αE can also be interpreted as the effect of bending stiffness of the membrane, since both compressive and bending stiffness are functions of the Young's modulus.
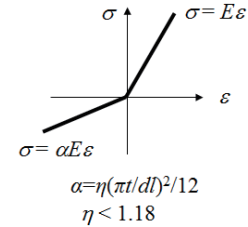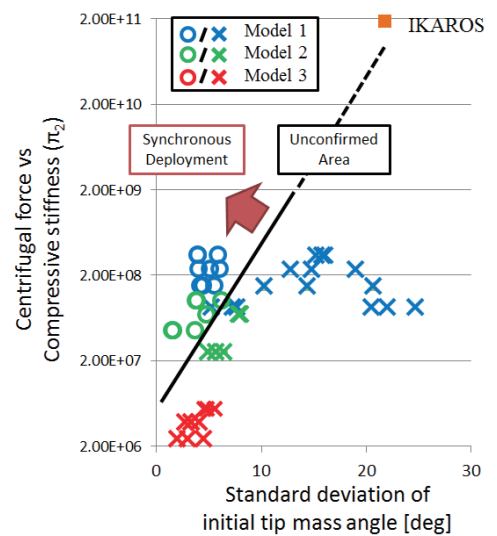
The dimensionless analysis of the experimental results shows that the initial imbalanced shape has an effect to the deployment synchronicity. The dimensionless numbers π_2 under the experimental condition and the IKAROS's condition are plotted in Fig. 22. The vertical axis means the dimensionless number π_2 and horizontal axis means a standard deviation of the initial tip mass angle before the second stage deployment. The plot points are figured by ○-mark or x-mark. The ○-mark means all the petals are deployed synchronously and the x-mark means the sail is deployed asynchronously. When the plot point is located in the upper area in the figure, the sail's deployment dynamics is affected by the centrifugal force largely against the crease stiffness. And when the plot point is located in the right area in the figure, the second stage deployment is started from the imbalanced cross shape. A black colored line means a boundary whether or not the deployment is synchronous; in other words, the deployment can be safely conducted.

Figure 22 shows that both dimensionless number π_2 and a standard deviation of the initial tip mass angle have clear relations to the deployment synchronicity. This is understood as follows. In the small scale experiment, a strong effect of membrane compressive stiffness was observed. As the initial shape becomes more imbalanced, the effect of the compressive stiffness will become more evident because the angle of "the double folding" becomes smaller in some petals. For this reason, the effect of the compressive stiffness becomes stronger as the standard deviation of the initial tip

mass angle becomes larger in Fig. 22. This hypothesis will be evaluated further in future research.

Furthermore, the dimensionless analysis of the experimental results provides some insights about the phenomena observed in IKAROS. Fig. 22 shows the point of IKAROS as a brown square. From the result, in case of IKAROS, the sail's deployment dynamics may be affected by the centrifugal force strongly, and the main cause of the asynchronous deployment may not be the sail's compressive stiffness or fold creases. But the second stage deployment was started from a significantly imbalanced cross shape as shown in Fig. 3. Thus, the effect of this imbalanced cross shape cannot be denied as one of the causes of IKAROS's asynchronous deployment in the second stage.

In an experiment that asynchronously deployed the membrane from imbalanced initial shapes, petal 1 that had the second largest initial tip mass angle delayed its deployment as shown in Fig. 18(a). This reason was assumed as the effect of plastic creases on the membrane in the scale model. Similarly, in IKAROS, the petal with the relatively large initial tip mass angle delayed its deployment significantly, as shown in Fig. 3 and Fig. 5. This reason may not be the plastic creases on the membrane, according to the present dimensionless analysis. In IKAROS, the centrifugal force was significantly higher than the membrane stiffness. Therefore, this analysis possibly suggests that there were other factors that caused the asynchronous deployment, such as small membrane strips to hold the membrane during the launch of IKAROS. Further study will address this issue.

Fig. 21.   Membrane's compressive stiffness[4].

Fig. 22.   Dimensionless number π_2 for the second stage deployment experiment.

5. Conclusions

This study described the problems of imbalanced membrane shape and deployment of IKAROS, and conducted deployment experiments with scaled models to clarify the reasons of the imbalances. The results were analyzed using the similarity laws, to make the following two findings.

First, the experiments suggested that IKAROS's imbalanced cross shape after the first stage deployment was significantly affected by sail length non-uniformity.

Second, the scale-down sail models' second stage deployment dynamics was observed to be affected by in-plane compressive stiffness. In addition, the dimensionless analysis suggests that when the second stage deployment was started from an imbalanced cross shape, the effect of compressive stiffness became larger. When this result is extrapolated to IKAROS, the following insights are obtained. IKAROS's second stage deployment dynamics was significantly affected by centrifugal force, unlike the small-scale experiment, instead of membrane's compressive stiffness. Therefore, this analysis may suggest the existence of other factors that might have caused the asynchronous deployment of IKAROS, such as membrane strips that held the sail during the launch.

Appendix A. Definitions of Symbols in Eqs. (1) and (2)

This appendix describes the definitions in detail of the bending stiffness of the membrane as a thin plate, D, and of the centrifugal forces provided by the tip masses, F. These symbols appear in Eqs. (1) and (2).

$$D = \frac{Et^3}{12\,(1-\nu^2)} \tag{3}$$

$$F = m_t\, r\, \omega^2 \tag{4}$$

where ν is the Poisson's ratio of the membrane, m_t is the total mass of the tip masses attached on the membrane model, r is the half of the diagonal length of the square membrane, or the distance from the center to the tip-mass attached points, and ω is the angular velocity of the membrane model during the deployment experiments, generated by the motor.

References

1) Mori, O., Sawada, H., Hanaoka, F., Kawaguchi, J., Shirasawa, Y., Sugita, M., Miyazaki, Y., Sakamoto, H and Funase, R.: Development of Deployment System for Small Size Solar Sail Mission, *Transactions of the Japan Society for Aeronautical and Space Sciences*, *Space Technology Japan*, **7**, ists26, (2009) pp. Pd_87-pd_94.

2) Shirasawa, Y., Mori, O., Miyaaki, Y., Sakamoto, H., Hasome, M., Okuizumi, N., Sawada, H., Matunaga, S., Furuya, H., and Kawaguchi, J.: Evaluation of Membrane Dynamics of IKAROS based on Flight Result and Simulation using Multi-Particle Model, *Transactions of the Japan Society for Aeronautical and Space Sciences*, *Space Technology Japan*, **10**, No. ists28,4-4, (2012)

3) Muta, A., Shintaku, K., Matunaga, S. and Okuizumi, N.: Experiment and Analysis of Membrane Deployment for Scale Model Solar Sail, ISTS2011, 2011-c-28, Okinawa.

4) Inoue, S.: Prediction Methods of Wrinkling in Thin-Membrane, ISTS2009, 2009-c-20s, Tsukuba.